Journal of Materials Chemistry C

Accepted Manuscript

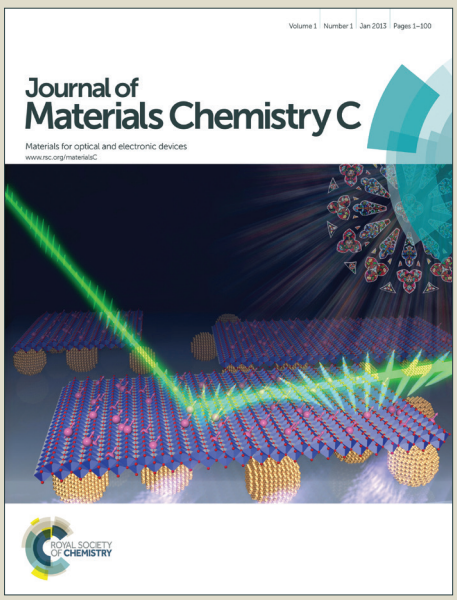

ROYAL SOCIETY OF CHEMISTRY

www.rsc.org/materialsC

Journal of Materials Chemistry C

Dynamic Article Links ►

Cite this: DOI: 10.1039/c0xx00000x

www.rsc.org/MaterialsC

Communication

Cashmere-derived keratin for device manufacturing on the micro- and nanoscale†

Benedetto Marelli,[a] and Fiorenzo G. Omenetto*[ab]

Received (in XXX, XXX) Xth XXXXXXXXX 20XX, Accepted Xth XXXXXXXXX 20XX

DOI: 10.1039/b000000x

Cashmere-derived keratin was extracted in water solution and then processed with a slow drying technique to obtain flexible, transparent, conformable optical elements. Using soft-lithography techniques, keratin film surfaces were micro- and nano-patterned to obtain biocompatible, compostable, microlens arrays and multidimensional diffractive gratings. Alternatively, keratin was assembled to form periodic three-dimensional nanostructures (i.e. inverse opals) to control and manipulate the flow of light through its lattices.

The technological quest for flexible devices to be interfaced with the biological world has driven the recent reinvention of biopolymers as substrates for electronic and photonic applications, to complement their more traditional use in the biomedical field.[1, 2] Specifically, biopolymer-based optics have not only shown the potential to perform on par with their "synthetic" counterpart and with inorganic materials, but have also displayed distinct features (e.g. stabilization of biochemically active molecules, biocompatibility, edibility, compostability) that have efficiently exploited the interface between photonics and biomedicine.[1, 3-8] However, only few materials have been shown to meet the stringent physical properties (transparency, conformability, flexibility and nanometric surface roughness) and the limited processing conditions (i.e. water-based and within physiological ranges) needed to design biofunctional, 'green' devices, resulting in a shortage of material choice that restricts the applicability of biopolymer-based photonic.

Here, we present cashmere-derived keratin films as technological materials by adopting simple processing techniques and micro- and nanofabrication approaches (Fig. 1). We use 2D and 3D photonic devices as benchmarks to validate the effectiveness of this manufacturing approach. The use of keratin-based materials is strongly entrenched within our history, with humans using horns as tools in the upper paleolithic and wool in the late Neolithic. The interest in high-tech keratinous materials is only recent and has been spurred by the vision of converting abundant keratin-based byproducts from the farming (chicken feathers, cow hooves) and textile (e.g. hair, wool, cashmere) industries into advanced materials.[9] Despite the numerous successes in the use of keratin for biomedical applications,[10-14] keratin films suffer from unfavorable mechanical properties (i.e. brittleness), which have spurred research on optimizing its material properties.[15-19] The brittleness of regenerated keratin originates from the protein's amino acidic content. The distinct, high concentration of cysteine, which governs the protein's self-assembly, (from 2 to 18 wt%) imparts the formation of intra- and inter-molecular crosslinks (i.e. disulphide bonds) ultimately stiffening the protein structure.[20]

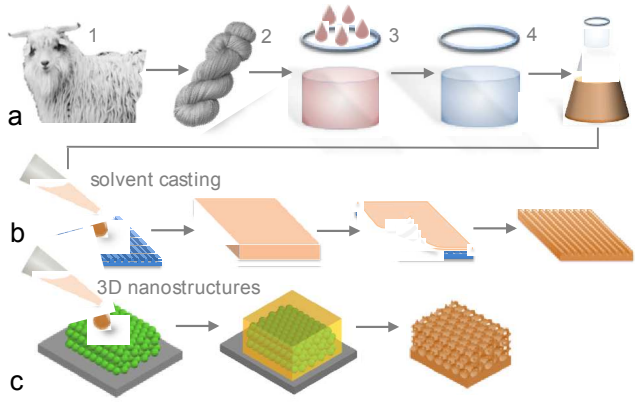

Figure 1. Fabrication steps of keratin-based photonic material. a) Optical grade keratin aqueous solution is obtained by extracting keratin from the fibers of cashmere goat-derived wool. b) Keratin optical elements are fabricated through solvent-casting of keratin solution on polydimethylsiloxane-made patterned molds (e.g. diffraction grating). c) Fabrication of keratin photonic crystals is obtained by infiltrating a pre-formed PMMA-made opal with keratin solution on a silicon wafer. Upon drying, acetone is used to dissolve the PMMA opal and to detach the nanostructured free-standing keratin film from the silicon wafer, resulting in the formation of a keratin inverse opal structure.

Conversely, the concurrent formation of intermolecular hydrogen bonds, which enables flexibility in wool fiber, is limited in the regenerated material.[21] Indeed, keratin has been plasticized by increasing the non-bound water content through doping with hygroscopic salts (e.g. $MgCl_2$)[15] and polyols (i.e. glycerol)[22] or blending with hygroscopic synthetic polymers (i.e. polyethylene oxide)[23]. Alternatively, keratin flexibility in the dried state was enhanced by hybridization with highly conformable natural polymers such as silk fibroin[24, 25] or chitosan,[26] or by using thermally regulated processing techniques (i.e. heated compression molding). Post-extraction reduction (to kerateine) [13] or oxidation (to keratose)[27] of keratin cysteine groups has also been pursued to further modulate formation of disulphide groups

and to ultimately control the protein's physical (solubility, hydrophobicity, strength) and biological (resistance to pH, proteolythic and hydrolytic degradation) properties.

As an alternative route for keratin films processing, we propose to modulate keratin self-assembly and to ultimately improve the formation of intermolecular hydrogen bonds by a slow solution drying technique (Fig.1). Slow drying in various atmospheres is a recently proposed technique that induces ordered self-assembly and drives formation of oriented hydrogen bonds in organic and inorganic colloidal systems by slow addition of colloids around a pre-formed nucleus.[28] We hypothesize that slow evaporation of keratin solution under increasing relative humidity (RH) would enhance the formation of intermolecular hydrogen bonds during the disulphide bond-driven self-assembly process. To test this hypothesis, we then started by assessing the quality of the cashmere-derived keratin regeneration process. Cashmere was chosen as source of keratin due to the smaller diameter of the fiber when compared to other hair sources (e.g. merino wool or hair), which allows for a faster purification process. The molecular weight of cashmere-derived keratin was studied by sodium dodecyl-sulfate polyacrylamide gel electrophoresis (SDS-PAGE) in combination with Coomassie Brilliant Blue R-250 staining, according to a previously published protocol.[14] In Figure S1 a representative SDS-PAGE pattern of cashmere-derived regenerated keratin is shown, where a wide band in the range of 40-60 kDa is present, as previously described.[29] This large band (which is often split in two bands at 45-50 kDa and 55-60 kDa for different sources of keratin, e.g. human hair) has been attributed to the presence of type I and II alpha keratins.[10] Keratin with a predominant □-helical structure was also observed through the spectroscopic investigation of Amide I peak of the protein spectra obtained with FTIR (Amide I peak centered at 1651 cm^{-1}) and Raman (Amide I peak centered at 1646 cm^{-1}) analysis (Fig. 2 a and b, respectively).[30] Additionally, SDS-PAGE of cashmere-derived regenerated keratin showed the presence of a protein fraction of low molecular weight, with the band below 17 kDa, which has been reported as being a distinct signature for akeratin type II intermediate filaments and keratin high-sulfur matrix protein.[29] The cashmere-derived keratin solution was then drop casted at increasing relative humidity the properties of the so formed films (thickness≅80±7 □m) were tested upon conditioning at RH=30% for 24 hours. ATR-FTIR analysis depicted a RH-dependent change in the protein structure since higher RH levels corresponded to enhanced formation of helical structure (blue shift of the Amide I resonance from 1651 to 1653 cm^{-1})[25, 31] and increased crystallinity index (Amide III 1265/1235 cm^{-1} ratio from 0.79 to 0.83) (Fig.2a). Additionally, changes in the asymmetric and symmetric S-O stretching vibrations of the Bunte salts residues (1200-1000 cm^{-1}) indicated a RH-dependent modification of the S-O resonance, which may also suggest an alteration of the protein self-assembly.[25, 32, 33] μRaman analysis was used to quantify the Raman I_{850}/I_{830} ratio, expressed by the intensity values of 850 and 830 cm^{-1} doublet, to investigate the effects of keratin slow drying on the hydrogen-bonding state of protein's tyrosine phenoxyl group, which can be used as an indicator of tyrosine-mediated hydrogen bonds formation (Fig 2b).[33] In general, the higher the I_{850}/I_{830} ratio, the more hydrophobic is the tyrosine environment, corresponding to a decrease of the amount of hydrogen bonds formed.[33, 34] As the I_{850}/I_{830} ratio in keratin films decreased by increasing RH during drying (I_{850}/I_{830} ≈ 1.6 at RH=30%, 1.4 at RH=50%, 1.2 at RH=75%, 0.7 at RH=90% and 0.6 at RH=95%), we speculate that tyrosines experienced a more hydrophilic environment which likely led to hydrogen-bond formation.

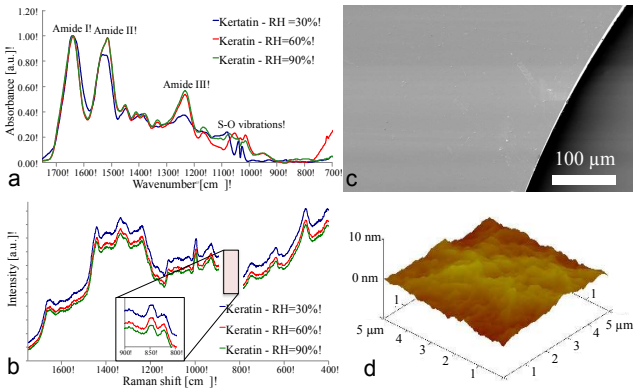

Figure 2. Chemical and morphological characterization of keratin films. a) ATR-FTIR spectra of keratin films casted at increasing RH values (i.e. blue line for RH=30%, red line for RH=60% and green line for RH=90%) showing differences in the protein conformation. In particular, the higher RH, the higher the crystallinity index (Amide III 1265/1235 cm^{-1} ratio). Additionally, RH-dependent changes in the S-O vibrations of the Bunte salts residues (1200-1000 cm^{-1}) suggest that the slow drying technique induced conformational changes in the protein. b) □-Raman spectra of keratin films casted at increasing RH values indicated a RH-dependent decrease in the full width at half-maximum of the Amide I peak, suggesting that slow drying induced the self-assembly of keratin molecules into more ordered structures. Additionally, the RH-dependent decrease in the I_{850}/I_{830} ratio indicated that the tyrosines experienced a more hydrophilic environment during slow drying, and that they were involved in hydrogen-bond donation. c) Representative SEM micrograph of keratin films depicting the homogenous surface of the material obtained by solvent-casting technique. d) Representative AFM micrograph of the surface morphology of solvent-casted keratin films depicting a roughness of approximately 10 nm.

To further investigate the effects of slow-drying process on the keratin structure, the concentration of free thiol groups (i.e. reduced cysteine) in the assembled films as a function of the relative humidity used in the slow-drying process was measured according previously reported methodology based on Ellman's reagent.[10] In general, the higher the concentration of reduced cysteine in the protein, the lower the crosslinking, as the cysteine thiol group is oxidize in the formation of disulphide bonds. As reported in Table S1, an RH-dependent increase in the amount of reduced cysteine present in the assembled keratin film was measured, which indirectly indicated the formation of fewer crosslinking bonds in the films assembled at increasing RH. Interestingly, the aqueous solution of cashmere-derived keratin possessed an increased amount of reduced cysteine when compared to previously published results obtained from hair-extracted regenerated keratin. Indeed, keratin self-assembly was seen to be affected by the slow drying process, which facilitated formation of tyrosine-mediated hydrogen bonds within the protein. Keratin film flexibility was then empirically evaluated by wrapping rectangular films (t=73±7 □m, l_1=45±1 mm, l_2=80±1 mm) around stainless steel rods of decreasing diameter d

(5mm< d <20 mm). Keratin solution casted at RH = 30 and 50 and 75% yielded films that were too brittle to be handled. In great contrast, slow drying of keratin solution at RH=85 and 95% produced films that were bendable around ∅=20 and 7 mm rods, respectively, which can be correlated with the decreased number of disulphide crosslinking bonds formed for film assembled at increasing RH . Importantly, the distinct flexibility of keratin films dried at RH ≥ 85% was not temporary, as the films properties remained unchanged for at least one year.

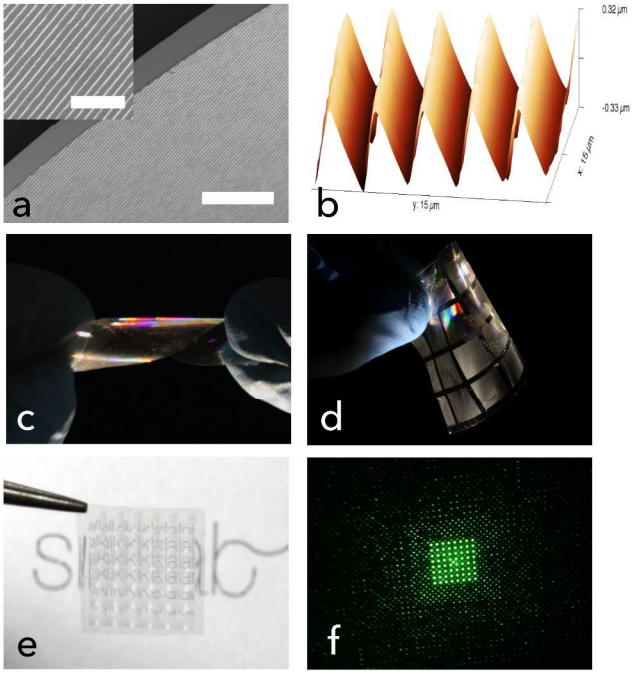

Figure 3. Different keratin optical elements. a) SEM micrograph and b) AFM image of a keratin-made diffraction grating (l=2400 l/mm). c) Photograph depicting the flexibility of a keratin-made diffraction grating. d) Photograph of multiple optical elements in a single, free standing keratin-made film (master from Digital Optics Inc., Tessera Corporation). e) a 6 × 6 keratin lens array. f) Photograph of a projected pattern obtained from propagation of a green light laser source through 2D diffraction patterns. The images are taken at a distance of 10 cm from the keratin optical element.

Cashmere-derived keratin films resulted transparent (90±3% transmissive) to visible light spectrum (400-700 nm) (Fig 2c) with an index of refraction (*n*) of 1.56 (at □=633 nm), independent of the drying-process indicating that the different (process-dependent) protein conformations did not affect the material's optical properties, consistent with previously reported measurements obtained from keratin transparent films (90-95% transmissive)[10] and from feather-extracted keratin (n=1.56-1.58)[15]. Additionally, keratin films light transmission across the visible spectrum and refractive index were similar to the ones reported for regenerated silk fibroin films (90-95% transmissive and n=1.55),[7] indicating converging optical properties for two biopolymers that share the amino-acidic nature, a similar self-assembly pathway and a structural functionality outside the body. Analogously, casting of keratin film on a polydimethylsiloxane (PDMS) surface molded on a fused quartz wafer yielded a root-mean-square (RMS) surface roughness of 7±2 nm, which was not affected by slow drying processing and that is in the same order of surface roughness measured for silk fibroin films.[7]

The promising transparency, low surface roughness, and flexibility results provided the basis for application of slow-drying processing to fabrication of keratin-based diffractive optical elements (Fig. 3). Keratin solution was casted on previously used PDMS-made patterned diffractive optical surfaces, including holographic diffraction gratings with varying line pitches, and dried at 95% RH (Fig. 3a and b). Upon acclimation at room conditions for 30 minutes, keratin films were separated from the grating masks through mechanical lifting. Only films with thickness higher than 40 □m were robust enough to be lifted. For material characterization and analysis, keratin films were fabricated with a standard 70 □m thickness to match film flatness post-lifting, optical clarity and ease of handling. Morphological characterization with scanning electron and atomic force microscopies showed that solvent casting of keratin solution onto patterned PDMS masters resulted in conformal replicas of the substrate topography. The minimum feature that was replicated was in the order of tens of nanometers, which is optically relevant, as many optical elements are nanostructured with a periodicity in the order the visible wavelength. For 2400 l/mm diffraction grating masks, smooth, regularly patterned surfaces were visible with SEM and AFM, with grooves that were 200 wide (FWHM) and with wall roughness of approximately 10 nm (Fig. 3 a and b). In addition to diffractive gratings, keratin solution was casted on microlens arrays and on and phase masks gratings, to further investigate the ability to fabricate functional keratin-based optical elements (Fig. 3 c and d and Fig. S2).

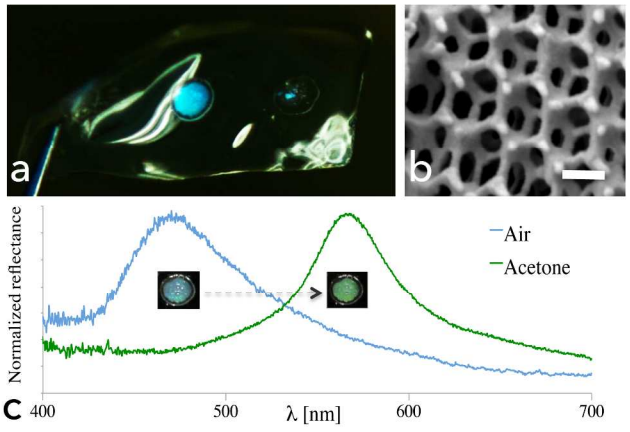

Figure 4. Keratin inverse opal and relative optical response. a) Picture of a keratin inverse opal (□=240 nm) embedded in a keratin film. b) SEM micrograph of the keratin-made inverse opal depicting the typical 3D lattice. Scale bar = 200 nm. c) Measured reflectance spectra obtained from a □=240 nm inverse opal. A redshift occurred upon infiltration of acetone in the opal. The inset images show a photograph taken under white-light illumination in air (left) and acetone (right), showing the visible change in structural color. Images were captured perpendicularly to the keratin film.

Additionally, optically relevant 3D structures were explored by using keratin to generate inverse opals. These wavelength-scale lattices can control the propagation of light resulting in structural color.[35] Structural coloration has been adopted in many organisms as a mean of social and sexual communication signals.[36] Plants, insects, birds, and marine animals have evolved

to organize biopolymers as chitin, melanin, keratin and cellulose in nanostructures to produce photonic architectures.[37] Opals and inverse opals (i.e. air-sphere lattices within a dielectric material) are examples of three-dimensional photonic crystals found in some species of weevils[38] and butterflies[39]. Analogous synthetic architectures have been proposed in the 1980s for the fabrication of nanoporous materials that control and manipulate the flow of light through their lattices, offering a compelling material functionalization for decorative, security, sensing and catalytic applications.[40] Recently, regenerated silk fibroin extracted from *Bombyx mori* cocoons has been proposed as biopolymer to fabricate functionalized, biocompatible and bioresorbable free-standing inverse opals to be used for pasmonics, biosensing and drug delivery.[4] Here, we adapted the previously reported template method based on the use of self-assembled poly(methyl methacrylate, PMMA) nanospheres (d=250 nm) infiltrated by a biopolymer solution to fabricate inverse opals entirely composed of regenerated keratin (KIO, Fig. 1 and Fig. 4). Keratin solution was poured into the PMMA template and allowed to solidify into a freestanding keratin film through slow solution drying at RH=95%. Keratin films were then transferred in acetone at 40ºC to dissolve PMMA spheres and to detach the biopolymer from the silicone waver used as substrate, resulting in the appearance of blue iridescence within the transparent keratin film (Fig. 4a). SEM analysis of the area of the films characterized by structural color confirmed the presence of an inverse-opal structure (□=235 nm), depicting a keratin lattice with air-voids of dimension slightly smaller than the diameter of the PMMA nanospheres used as template (Fig. 4b). The high-resolution SEM micrograph also showed a smooth keratin nanostructure, well different from the aggregated nanoparticles that comprised previously reported keratin films obtained from human hair.[10, 14] Nonetheless, the lattice had some imperfections and the average dimension of the air gaps was disperse between 220 and 250 nm, likely attributable to the properties of the protein that is comparatively more brittle than other biopolymers (e.g. silk fibroin). Additionally, the acetone treatment had a detrimental effect on the flexibility of keratin films, which became brittle, probably due to the dehydration that occurred during the process and the consequent increase in crosslinking. The number of reduced cysteine in keratin films assembled at RH=95% decreased by a factor of circa 2 upon exposure to acetone (concentration of free thiol groups from 0.579±0.074 mM to 0.302±0.027 mM), which was an indirect indication of an increased formation of disulphide bonds and therefore of crosslinking. Further exposure to water or to water vapors did not reverse this acetone-driven crosslinking process. The optical response of KIOs was also evaluated through measurement of the reflected spectrum from the opal at normal incidence and by varying the index contrast of the opal by infiltrating the structure with acetone to cause a color shiftb decreasing the index contrast from □n≈0.56 to □n≈0.20. The observed blue reflectance spectrum from the KIO shifts to longer wavelengths when the index contrast decreases as illustrated in Fig. 4c, which illustrates a transition from a center wavelength □=469 nm, to □=565 nm upon acetone infiltration. The reflectance spectrum of KIO ($FWHM_{KIO}$ = 63 nm) was found to be broader to comparable opals manufactured with silk ($FWHM_{SIO}$ = 48 nm)[4] further underscoring the added irregularity of the bulk inverse opal structure observed in the electron microscopy images, where the presence of imperfections in the lattice of KIOs contributes to a broader spectral response (or a less defined pseudo-bandgap). Nevertheless, the ability to obtain of three-dimensional nanostructured photonic crystals with regenerated keratin enables the use of this protein as a material for the fabrication of biocompatible, degradable, and potentially implantable spectral elements that can be used within biological tissues to provide non-endogenous spectral signatures.

These results open the door to additional opportunities for keratin-based biomaterials, which are predicated on the directed self-assembly of the protein by a simple slow solution drying process. Control over protein structure, self-assembly and organization on the mesoscale is a key aspect in the development of structural protein-based technology. In this study, slow-drying induced control over protein self-assembly have shown a flexible, conformable, transparent material, which can be formed in an all-water environment and that can be nanopatterned through soft-lithographic techniques or can be assembled in three-dimensional photonic crystals. Keratin is a family of structural proteins that have a structural role both inside and outside the body. This dual nature makes keratin a protein of interest both for in vivo and ex vivo applications. Given keratin's demonstrated degradation through proteolytic activity[12, 13], these studies may enable the fabrication of keratin-based optical devices to be implanted in the body. For environmental applications, keratin-based devices may be dispersed in the ambient without the need to be retrieved at a later time point, expanding the material options for transient devices for sensing and detection systems.[41]

Conclusions

In the present manuscript, we reported a methodology to enhance the properties of cashmere-derived keratin-based films by simply modulating the environmental conditions at which the regenerated protein is exposed during solvent-casting. Slow drying techniques can be applied to cashmere-derived keratin in an aqueous environments and at room temperature to obtain flexible, transparent, conformable films.

Such films can be easily patterned on the micro and nanoscale. Soft-lithography techniques can be applied to impart micro- and nano-sized topographies on the surface of the films, yielding diffractive optical elements. Template-assisted self-assembly of keratin can also be used to form periodic three-dimensional nanostructures in the form of photonic crystals (i.e. inverse opals) that exhibit structural color.

Acknowledgements

The authors would like to acknowledge support through an NSF-INSPIRE grant (DMR-1242240).

Notes and references

[a] *Department of Biomedical Engineering, Tufts University, 4 Colby St., Medford, MA, 02155, USA. Fax: +1 617 627 3231; Tel: +1 617 627 4972; E-mail: fiorenzo.omenetto@tufts.edu;*

[b] *Department of Physics, Tufts University, 4 Colby St., Medford, MA, 02155, USA. Fax: +1 617 627 3231; Tel: +1 617 627 4972;*

† Electronic Supplementary Information (ESI) available: [details of any supplementary information available should be included here]. See DOI: 10.1039/b000000x/

1. F. Omenetto and D. KapLan, *Nature Photonics*, 2008, 2, 641-643.
2. F. G. Omenetto and D. L. Kaplan, *Science*, 2010, 329, 528-531.
3. H. Tao, D. L. Kaplan and F. G. Omenetto, *Advanced Materials*, 2012, 24, 2824-2837.
4. S. Kim, A. N. Mitropoulos, J. D. Spitzberg, H. Tao, D. L. Kaplan and F. G. Omenetto, *Nature Photonics*, 2012, 6, 817-822.
5. K. Tsioris, G. Tilburey, A. Murphy, P. Domachuk, D. Kaplan and F. Omenetto, *Advanced Functional Materials*, 2010, 20, 1083-1089.
6. S. Parker, P. Domachuk, J. Amsden, J. Bressner, J. Lewis, D. Kaplan and F. Omenetto, *Advanced Materials*, 2009, 21, 2411-+.
7. B. D. Lawrence, M. Cronin-Golomb, I. Georgakoudi, D. L. Kaplan and F. G. Omenetto, *Biomacromolecules*, 2008, 9, 1214-1220.
8. P. Domachuk, H. Perry, J. J. Amsden, D. L. Kaplan and F. G. Omenetto, *Applied Physics Letters*, 2009, 95.
9. M. B. Dickerson, A. A. Sierra, N. M. Bedford, W. J. Lyon, W. E. Gruner, P. A. Mirau and R. R. Naik, *Journal of Materials Chemistry B*, 2013, 1, 5505-5514.
10. S. Reichl, M. Borrelli and G. Geerling, *Biomaterials*, 2011, 32, 3375-3386.
11. M. Borrelli, S. Reichl, Y. Feng, M. Schargus, S. Schrader and G. Geerling, *Journal of Materials Science: Materials in Medicine*, 2013, 24, 221-230.
12. J. G. Rouse and M. E. Van Dyke, *Materials*, 2010, 3, 999-1014.
13. P. Hill, H. Brantley and M. Van Dyke, *Biomaterials*, 2010, 31, 585-593.
14. S. Reichl, *Biomaterials*, 2009, 30, 6854-6866.
15. T. Fujii and Y. Ide, *Biological and Pharmaceutical Bulletin*, 2004, 27, 1433-1436.
16. K. Katoh, M. Shibayama, T. Tanabe and K. Yamauchi, *Biomaterials*, 2004, 25, 2265-2272.
17. R. Li and D. Wang, *Journal of Applied Polymer Science*, 2013, 127, 2648-2653.
18. H. Xie, S. Li and S. Zhang, *Green Chemistry*, 2005, 7, 606-608.
19. A. Aluigi, M. Zoccola, C. Vineis, C. Tonin, F. Ferrero and M. Canetti, *International Journal of Biological Macromolecules*, 2007, 41, 266-273.
20. W. Shi and M. J. Dumont, *Journal of Materials Science*, 2014, 49, 1915-1930.
21. C. Popescu and H. Höcker, in *International Review of Cell and Molecular Biology*, ed. W. J. Kwang, Academic Press, 2009, vol. Volume 277, ch. 4, pp. 137-156.
22. K. Yamauchi, A. Yamauchi, T. Kusunoki, A. Kohda and Y. Konishi, *Journal of Biomedical Materials Research*, 1996, 31, 439-444.
23. C. Tonin, A. Aluigi, C. Vineis, A. Varesano, A. Montarsolo and F. Ferrero, *J. Therm. Anal. Calorim.*, 2007, 89, 601-608.
24. Y. Iridag and M. Kazanci, *Journal of Applied Polymer Science*, 2006, 100, 4260-4264.
25. A. Vasconcelos, G. Freddi and A. Cavaco-Paulo, *Biomacromolecules*, 2008, 9, 1299-1305.
26. T. Tanabe, N. Okitsu, A. Tachibana and K. Yamauchi, *Biomaterials*, 2002, 23, 817-825.
27. R. C. de Guzman, M. R. Merrill, J. R. Richter, R. I. Hamzi, O. K. Greengauz-Roberts and M. E. Van Dyke, *Biomaterials*, 2011, 32, 8205-8217.
28. Y. H. Lee, Y. L. Yang, W. C. Yen, W. F. Su and C. A. Dai, *Nanoscale*, 2014, 6, 2194-2200.
29. M. Yokohama, T. Masuda, T. Amano, H. Hirayama and T. Manabe, *Animal Science Journal*, 2004, 75, 401-405.
30. A. Pielesz and A. Wesełucha-Birczyńska, *Journal of Molecular Structure*, 2000, 555, 325-334.
31. J. Koga, K. Kawaguchi, E. Nishio, K. Joko, N. Ikuta, I. Abe and T. Hirashima, *Journal of Applied Polymer Science*, 1989, 37, 2131-2140.
32. F. Selmin, F. Cilurzo, A. Aluigi, S. Franzè and P. Minghetti, *Results in Pharma Sciences*, 2012, 2, 72-78.
33. G. J. Thomas Jr, *Biopolymers - Biospectroscopy Section*, 2002, 67, 214-225.
34. G. Freddi, A. Anghileri, S. Sampaio, J. Buchert, P. Monti and P. Taddei, *Journal of Biotechnology*, 2006, 125, 281-294.
35. E. Yablonovitch, *Physical Review Letters*, 1987, 58, 2059-2062.
36. H. W. Yin, B. Q. Dong, X. H. Liu, T. R. Zhan, L. Shi, J. Zi and E. Yablonovitch, *Proceedings of the National Academy of Sciences of the United States of America*, 2012, 109, 10798-10801.
37. P. Vukusic and J. R. Sambles, *Nature*, 2003, 424, 852-855.
38. A. R. Parker, V. L. Welch, D. Driver and N. Martini, *Nature*, 2003, 426, 786-787.
39. A. L. Ingram and A. R. Parker, *Philosophical Transactions of the Royal Society B: Biological Sciences*, 2008, 363, 2465-2480.
40. P. Russell, *Science*, 2003, 299, 358-362.
41. S.-W. Hwang, H. Tao, D.-H. Kim, H. Cheng, J.-K. Song, E. Rill, M. A. Brenckle, B. Panilaitis, S. M. Won, Y.-S. Kim, Y. M. Song, K. J. Yu, A. Ameen, R. Li, Y. Su, M. Yang, D. L. Kaplan, M. R. Zakin, M. J. Slepian, Y. Huang, F. G. Omenetto and J. A. Rogers, *Science*, 2012, 337, 1640-1644.

Cashmere-derived keratin is extracted in water solution and then processed with slow drying technique to obtain flexible, transparent, conformable optical elements.
136x124mm (300 x 300 DPI)